

## Chemomechanical oscillations in a responsive gel induced by an autocatalytic reaction

Kai Li,<sup>1</sup> Peiyi Wu,<sup>2</sup> and Shengqiang Cai<sup>2,3,a)</sup>

<sup>1</sup>Department of Civil Engineering, Anhui Jianzhu University, Hefei, Anhui 230601, People's Republic of China

<sup>2</sup>State Key Laboratory of Molecular Engineering of Polymers, Fudan University, Shanghai 200433, People's Republic of China

<sup>3</sup>Department of Mechanical and Aerospace Engineering, University of California, San Diego, La Jolla, California 92093, USA

(Received 8 June 2014; accepted 15 July 2014; published online 30 July 2014)

In this article, we investigate dynamic behaviors of a gel layer attached to a rigid substrate and submerged in a continuous stirred tank reactor. With a continuous feed of fresh reactants in the reactor, the concentrations of reactants stay constant on the surface of the gel layer. However, the concentrations of reactants inside the gel are inhomogeneous and vary with time, which are determined by the diffusion and chemical reactions of the reactants. Additionally, both monotonic and oscillatory swelling-shrinking dynamics are predicted in the gel if the swelling capability of the gel depends on the concentration of a reactant. Based on autocatalytic reaction, kinetic model, and nonequilibrium thermodynamic theory of gels, in this article, we investigate the effect of the thickness of the gel layer, lateral prestretches in the gel and the initial concentrations of reactants in the gel on its dynamic behaviors. We have also calculated the evolution of the swelling force that the gel layer exerts on its constrained substrate. The results of this article may find potential applications in using responsive gels to make chemo-mechanical sensors, actuators, biomimetic devices, and even drug delivery systems. © 2014 AIP Publishing LLC.

[<http://dx.doi.org/10.1063/1.4891520>]

### I. INTRODUCTION

Submerged in an environment containing solvent, a polymer network imbibes the solvent and swells, resulting in a gel. Depending on the functional groups tethered to the polymer chain, the amount of swelling in the gel may change significantly with a small variation of environmental temperature,<sup>1</sup> pH value,<sup>2</sup> electric field,<sup>3</sup> and concentrations of ions.<sup>4</sup> Using responsive gels, different research groups have successfully designed and fabricated diverse soft active devices and systems.<sup>5–7</sup>

Recently, many intriguing phenomena associated with the interaction between chemical reactions and deformations in hydrogels have been discovered and investigated.<sup>8</sup> For example, by incorporating a transition metal catalyst Ru(bpy)<sub>3</sub> moiety into polymer chains, a self-oscillating reaction, named Belousov–Zhabotinsky (BZ) reaction, can happen in a gel.<sup>9</sup> During the course of the reaction, the concentrations of Ru(bpy)<sub>3</sub><sup>2+</sup> and Ru(bpy)<sub>3</sub><sup>3+</sup> in the gel oscillate, which may induce cyclic swelling-shrinking changes<sup>10</sup> or peristaltic motion in the gel.<sup>11,12</sup> The synthetic self-oscillating BZ-reaction gels have been explored to emulate various biological functions<sup>13,14</sup> and realize pulsatile drug delivery.<sup>15</sup> Based on the kinetics of self-oscillating reactions and the thermodynamics of gels, both theoretical and numerical models have been proposed to explain diverse phenomena observed in BZ-reaction gels.<sup>16–18</sup>

Oscillating dynamics observed in BZ-reaction gels are the direct consequences of BZ-reactions. Nevertheless, several recent experiments have shown that through the coupling between large deformation in a chemical responsive gel and bistable autocatalytic chemical reactions, which are much more common than self-oscillating reactions, various dynamic behaviors, including oscillations, can also be realized in the gel system. In the experiment, a chemically responsive gel is submerged in a continuous stirred tank reactor (CSTR), where an autocatalytic reaction proceeds (Fig. 1).<sup>19–26</sup> In a CSTR, with a continuous feed of fresh reactants, the autocatalytic reaction with long induction time is kept in its initial unreacted state. However, the state of reactants inside the gel is determined by the reaction rate and diffusion process, and the concentrations of reactants are usually not homogeneous and vary with time. Depending on the size of the gel, the reactants in the gel can be either in unreacted state with low concentration or reacted state with high concentration steadily.<sup>27,28</sup> In particular, for a gel with intermediate size, both reacted and unreacted states of the reactants in the gel can be steady, which is known as spatial bistability.<sup>27,28</sup> Furthermore, if the gel is responsive to the concentration of a reactant, by simply changing the size of the gel or prestretches in the gel, various swelling-shrinking dynamics of the gel can be observed.<sup>24</sup>

According to our knowledge, Boissonade *et al.*<sup>28,29</sup> are the first, who combine reaction-diffusion kinetics model of reactants and thermodynamics of gels to interpret the oscillation of a free-standing responsive gel in a CSTR. However, in most applications, gels are either partially constrained by

<sup>a)</sup>Electronic mail: shqcai@ucsd.edu

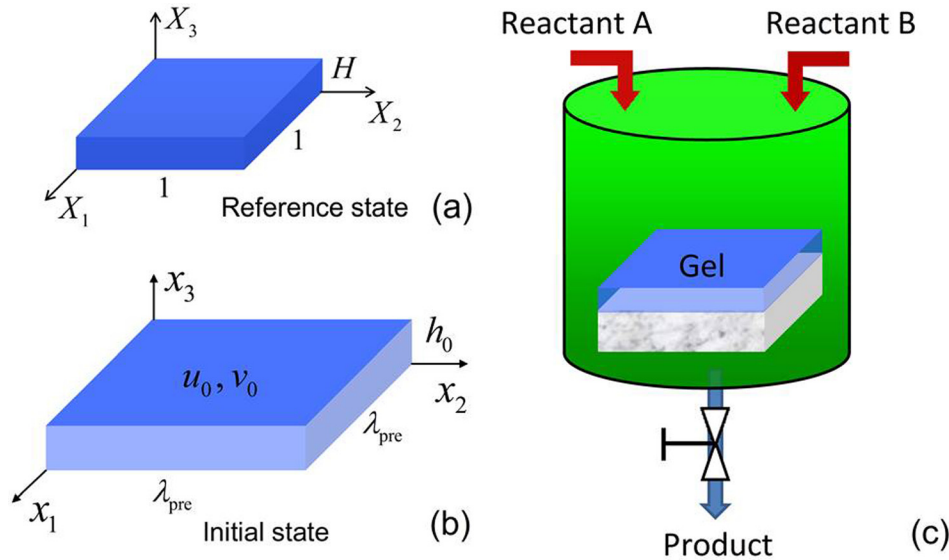


FIG. 1. Schematics of the gel layer in (a) reference state and (b) initial state.  $H$  is the thickness of the gel layer in dry state,  $\lambda_{pre}$  is the lateral prestretch,  $h_0$  is the initial thickness of the gel,  $u_0$  and  $v_0$  are normalized initial concentrations of reactants in the gel. (c) is a schematic of a chemically responsive hydrogel layer bonded on a rigid impermeable substrate in a CSTR. The upper surface of the hydrogel layer is in contact with the solution in the reactor. In the reactor, an autocatalytic CT reaction proceeds.

substrates or subject to mechanical forces.<sup>30</sup> Furthermore, the forces that swelling gels exerts on their constraints are often used to actuate structures and trigger deformations. Therefore, in this paper, we combine kinetic model of autocatalytic reactions, poroelasticity theory developed by Biot<sup>31</sup> and other researchers,<sup>32</sup> and thermodynamics of gels formulated by Flory<sup>33</sup> to compute deformation field, stress distribution, and the reactant concentrations in the gel, which is submerged in a CSTR and constrained by a rigid impermeable substrate (Fig. 1). In particular, we uncover the influence of gel thickness, lateral prestretches, and the initial concentrations of reactants on the dynamic behaviors of the gel. We have also calculated the evolution of the swelling force, the gel layer exerts on the constraint. We hope the results of the paper would promote the understanding of the coupling between chemical reactions and finite deformation in soft materials, and find potential applications in controlling oscillations of chemo-responsive gels by mechanical ways.

## II. MODEL AND FORMULATION

Figure 1 sketches a chemically responsive hydrogel layer immersed in a CSTR. A dry gel layer, with the thickness  $H$  as shown in Figure 1(a), is first prestretched equal-biaxially in lateral directions and bonded to a rigid and impermeable substrate. The gel layer is then submerged in a solution and swells till equilibrium with the thickness  $h_0$ , which is viewed as initial state of the gel layer in this article (Fig. 1(b)). Finally, the gel layer is immersed in a CSTR, where autocatalytic reactions proceed. Based on our models, various swelling-shrinking behaviors of the gel layer can be predicted.

In the paper, the dry gel layer is taken to be the state of reference. Let  $X_1$  and  $X_2$  be the material coordinates in the plane of the dry gel layer, and  $X_3$  be the material coordinate normal to the layer (Fig. 1(a)). The substrate fixes the lateral stretches of the gel  $\lambda_1 = \lambda_2 = \lambda_{pre}$ . At time  $t$ , the marker  $X_3$  moves to a place  $x_3(X_3, t)$ . The vertical stretch is

$$\lambda_3(X_3, t) = \frac{\partial x_3(X_3, t)}{\partial X_3}. \quad (1)$$

The concentration of the solvent in the gel is also a time-dependent field,  $C(X_3, t)$ . The number of solvent molecules is conserved, so that

$$\frac{\partial C(X_3, t)}{\partial t} + \frac{\partial J(X_3, t)}{\partial X_3} = 0, \quad (2)$$

where  $J(X_3, t)$  is the nominal flux of the solvent in the vertical direction, i.e., the number of solvent molecules crossing unit area in the reference state per unit time.

The hydrogel layer is in mechanical equilibrium in the process of solvent migration, so that the stress in vertical direction vanishes

$$\sigma_3(X_3, t) = 0. \quad (3)$$

The hydrogel is not in diffusive equilibrium. The chemical potential of the solvent in the hydrogel is a time-dependent field,  $\mu(X_3, t)$ . The gradient of the chemical potential drives the solvent to migrate in the hydrogel. Following our previous work,<sup>33</sup> the flux is taken to be linear in the gradient of the chemical potential

$$J(X_3, t) = -\frac{CD}{\lambda_3^2 kT} \frac{\partial \mu(X_3, t)}{\partial X_3}, \quad (4)$$

where  $D$  is the diffusivity of the solvent and  $kT$  is the temperature in the unit of energy. The stretch  $\lambda_3$  in Eq. (4) is to account for the effect of deformation on solvent migration.

Since the concentrations of the reactants are generally small compared to the concentration of solvent, the volume of the reactants is ignored. The volume of the swollen gel is assumed to be equal to the sum of the volume of the dry polymer network and the volume of solvent in the gel, namely

$$1 + \Omega C = \lambda_{pre}^2 \lambda_3, \quad (5)$$

where  $\Omega$  is the volume per solvent molecule.

Using the free energy of a gel given by Flory and Rehner, the equations of state can be written as<sup>35</sup>

$$\frac{\sigma_1 \Omega}{kT} = \frac{N\Omega}{\lambda_{\text{pre}}^2 \lambda_3} (\lambda_{\text{pre}}^2 - 1) + \log \left( 1 - \frac{1}{\lambda_{\text{pre}}^2 \lambda_3} \right) + \frac{1}{\lambda_{\text{pre}}^2 \lambda_3} + \frac{\chi}{\lambda_{\text{pre}}^4 \lambda_3^2} - \frac{\mu}{kT}, \quad (6a)$$

$$\frac{\sigma_2 \Omega}{kT} = \frac{N\Omega}{\lambda_{\text{pre}}^2 \lambda_3} (\lambda_{\text{pre}}^2 - 1) + \log \left( 1 - \frac{1}{\lambda_{\text{pre}}^2 \lambda_3} \right) + \frac{1}{\lambda_{\text{pre}}^2 \lambda_3} + \frac{\chi}{\lambda_{\text{pre}}^4 \lambda_3^2} - \frac{\mu}{kT}, \quad (6b)$$

$$\frac{\sigma_3 \Omega}{kT} = \frac{N\Omega}{\lambda_{\text{pre}}^2 \lambda_3} (\lambda_3^2 - 1) + \log \left( 1 - \frac{1}{\lambda_{\text{pre}}^2 \lambda_3} \right) + \frac{1}{\lambda_{\text{pre}}^2 \lambda_3} + \frac{\chi}{\lambda_{\text{pre}}^4 \lambda_3^2} - \frac{\mu}{kT}, \quad (6c)$$

where  $N$  is the number of polymer chains in the gel divided by the volume of the dry polymers and  $\chi$  is a dimensionless measure of the enthalpy of mixing. From the above equations, we can know that the swelling capability of the gel decreases with increasing the value of  $\chi$ .

Depending on the functional group bonded with polymer chains, the swelling capability of a gel can vary significantly with the change of external stimuli. For example, the

linear swelling ratio of a polyelectrolyte gel can change as much as 10 times with a variation of ionic strength in the solution.<sup>36</sup> As another example, temperature-sensitive hydrogels such as PNIPAM gel can absorb or release a large amount of water by lowering or increasing the surrounding temperature.<sup>37,38</sup> Many models describing the responsiveness of different gels have been developed in the literature. Without losing generality, one of the simplest models for responsive gels is assuming that  $\chi$  is a function of the stimuli, such as the concentrations of ions, temperature, and so on.

In this paper, following Boissonade *et al.*,<sup>28,29</sup> to model the responsiveness of the gel, we assume  $\chi$  only depends on the concentration of one of the reactants in the solution:  $\text{H}^+$  in a sigmoidal function form

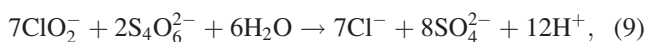
$$\chi(X_3, t) = \frac{\chi_{\text{max}} + \chi_{\text{min}}}{2} + \frac{\chi_{\text{max}} - \chi_{\text{min}}}{2} \tanh[s(v - v^*)], \quad (7)$$

where  $v$  is normalized concentration of  $\text{H}^+$ , which we will discuss more in the following paragraphs. In this paper, the parameters in Eq. (7) are chosen as  $\chi_{\text{min}} = 0.154$ ,  $\chi_{\text{max}} = 0.54$ ,  $s = 10$ , and  $v^* = 0.15$ . From Eq. (7), we know  $\chi$  is a monotonically increasing function of the concentration of  $\text{H}^+$ .

Substituting Eqs. (4)–(7) into Eq. (2), we arrive at a partial differential equation for the function  $\lambda_3(X_3, t)$

$$\frac{\partial \lambda_3}{\partial t} = D \frac{\partial}{\partial X_3} \left\{ \left( 1 - \frac{1}{\lambda_{\text{pre}}^2 \lambda_3} \right) \left[ \left( \frac{1}{(\lambda_{\text{pre}}^2 \lambda_3 - 1) \lambda_{\text{pre}}^2 \lambda_3^3} - \frac{2\chi}{\lambda_{\text{pre}}^4 \lambda_3^4} + \frac{N\Omega}{\lambda_{\text{pre}}^2 \lambda_3} \left( 1 + \frac{1}{\lambda_3^2} \right) \right) \frac{\partial \lambda_3}{\partial X_3} + \frac{1}{\lambda_{\text{pre}}^4 \lambda_3^3} \frac{\partial \chi}{\partial X_3} \right] \right\}. \quad (8)$$

The upper surface of the hydrogel layer (Fig. 1) is kept in contact with the solution in a CSTR. In the reactor, an autocatalytic Chlorite-Tetrathionate (CT) reaction proceeds. The reaction kinetics of the CT reaction can be well approximated by the following overall balance equation:<sup>27</sup>



and the reaction rate  $v_R$  is given by

$$v_R = -\frac{1}{7} \frac{d[\text{ClO}_2^-]}{dt} = k_0 [\text{ClO}_2^-] [\text{S}_4\text{O}_6^{2-}] [\text{H}^+]^2, \quad (10)$$

where  $k_0$  is the reaction rate constant. This above rate law exhibits quadratic autocatalysis in  $[\text{H}^+]$ , which can lead to spatial bistability.<sup>27</sup>

The flow rate in the CSTR is assumed to be large enough, so the concentrations of different species in the solution are assumed to be constant all the time. In the gel, the reaction-diffusion kinetics of different species are typically described by the following set of normalized equations:<sup>27</sup>

$$\frac{\partial u}{\partial t} = -u^2 v^2 + \nabla_{x_3}^2 u, \quad (11a)$$

$$\frac{\partial v}{\partial t} = \frac{12}{7} u^2 v^2 + \nabla_{x_3}^2 v. \quad (11b)$$

In the above equations, the concentrations of different species are normalized by the concentration of  $\text{ClO}_2^-$  at the surface of the gel:  $[\text{ClO}_2^-]_0$ , which is independent of time.  $u$  and  $v$  in Eq. (11) are normalized concentrations of  $\text{ClO}_2^-$  and  $\text{H}^+$ , respectively. In the reaction-diffusion system, an intrinsic length scale is introduced as  $l_0 = (D_1/2k_0)^{1/2}/([\text{ClO}_2^-]_0)^{3/2}$ , where  $D_1$  is the diffusivity of the reactants. Then, all length scales in the system are normalized by  $l_0$  and the time in the system is normalized as  $\tilde{t} = D_1 t/l_0^2$ . The typical values of these parameters are  $D_1 = 10^{-9} \text{m}^2 \text{s}^{-1}$ ,  $k_0 = 5 \times 10^6 \text{M}^{-3} \text{s}^{-1}$  and  $[\text{ClO}_2^-]_0 = 10^{-4} \text{M}$ , so  $l_0 = 1 \text{cm}$ .

At the surface of the constrained gel, the boundary conditions are

$$u(H, t) = u_{\text{ext}}, \quad (12a)$$

$$v(H, t) = v_{\text{ext}}, \quad (12b)$$

$$\mu(H, t) = 0, \quad (12c)$$

in which,  $u_{\text{ext}}$  and  $v_{\text{ext}}$  are the normalized concentrations of  $\text{ClO}_2^-$  and  $\text{H}^+$  in the bath reactor, respectively.

The rigid substrate is taken to be impermeable to the solvent and the reactants, so on the bottom surface of the gel layer, we have

$$\frac{\partial u(0, t)}{\partial X_3} = 0, \quad (13a)$$

$$\frac{\partial v(0, t)}{\partial X_3} = 0, \quad (13b)$$

$$\frac{\partial \lambda_3(0, t)}{\partial X_3} = 0. \quad (13c)$$

The initial conditions are

$$u(X_3, 0) = u_0, \quad (14a)$$

$$v(X_3, 0) = v_0, \quad (14b)$$

$$\lambda_3(X_3, 0) = \lambda_0, \quad (14c)$$

in which,  $u_0$  and  $v_0$  are the initial concentrations of  $\text{ClO}_2^-$  and  $\text{H}^+$  in the gel, respectively, and  $\lambda_0$  is the initial vertical stretch.

### III. RESULTS AND DISCUSSIONS

Using Matlab, we solve partial differential Eqs. (8) and (11) associated with boundary conditions (12), (13), and initial conditions (14). In the calculation, normalized crosslink density of the gel is fixed as  $N\Omega = 10^{-3}$  and the diffusivity of the solvent  $D$  is assumed to be equal to the diffusivity of reactants  $D_1$ . The concentration of  $\text{H}^+$  is fixed to be  $v_{ext} = 0.05$  on the top surface of the gel layer. In the following, we first explore how gel thickness  $H$ , initial concentrations of reactants, and lateral prestretch  $\lambda_{pre}$  affect the swelling-shrinking behaviors of the gel. We will also compute the evolution of stress field in the gel layer and swelling force that the gel layer exerts on the constrained substrate.

In Figure 2, we plot the evolution of the thickness of the gel with several thicknesses of the gel layer in the reference state,  $H$ . In the calculation, the lateral prestretch is fixed to be  $\lambda_{pre} = 3.0$ , and the initial concentrations of reactants in the gel are fixed to be  $u_0 = 0$ ,  $v_0 = 0.05$ . The initial vertical stretch of the gel layer in equilibrium can be calculated from Eq. (6c),  $\lambda_0 = 3.36$ . After contacting with the fresh reactants in the CSTR, the gel layer is not in equilibrium. Reactants

may migrate into or out of the gel with the progress of chemical reactions.

Figures 2(a)–2(c) plot three types of dynamic processes of gels with different thicknesses,  $H$ . For a gel layer with small thickness (Fig. 2(a)),  $H/l_0 = 0.5$ , the time for the  $\text{H}^+$  diffusing in the gel is much shorter than the characteristic time of chemical reactions, so the concentrations of the reactants inside the gel are very close to the concentrations of reactants in the external solution (Fig. 3(a)). Consequently, the gel layer shrinks very slightly and reaches a steady state in a short time.

However, for a gel with large thickness (Fig. 2(b)),  $H/l_0 = 2.2$ , the gel shrinks slowly and, finally, reaches a steady state with much smaller swelling ratio. This is because when the gel is thick, the diffusion of  $\text{H}^+$  in the gel needs much longer time compared to the chemical reaction, and the hydrogen ions in the gel are mostly in a reacted state. Due to the characteristics of autocatalytic reaction, compared to its initial state, the concentration of  $\text{H}^+$  is much higher in steady state (Fig. 3(b)).

For a medium thickness (Fig. 2(c)),  $H/l_0 = 0.9$ , the gel layer first shrinks to a state with small thickness and reacted  $\text{H}^+$  can migrate out of the gel within a short period, which decreases the value of  $\chi$  and makes the gel swell. After swelling, the thickness of the gel becomes large and  $\text{H}^+$  needs much longer time to migrate out of the gel, so the value of  $\chi$  increases and the gel shrinks back. In consequence, both the concentration of  $\text{H}^+$  (Fig. 3(c)) and the thickness of the gel layer keep oscillating and never reach steady state. It is worthwhile to point out that the oscillating behavior shown in the current system is a consequence of the coupling between large deformation of the gel and the autocatalytic reactions inside the gel, which is intrinsically different from the oscillating behaviors observed in BZ gels, where the chemical reactions are self-oscillating.<sup>9</sup>

Next, we investigate the influence of the initial concentrations of reactants on the swelling-shrinking behaviors of the gel layer. In the calculation, we change the initial concentrations of  $\text{ClO}_2^-$  to be  $u_0 = 0$  and  $\text{H}^+$  to be  $v_0 = 0.25$  in the gel, which is different from the initial concentrations of reactants in Figure 2. To compare with Figure 2(a), we set the same thickness of the gel layer  $H/l_0 = 0.5$  and lateral prestretch  $\lambda_{pre} = 3.0$  in Figure 4(a). Instead of shrinking, the gel layer swells initially, because the concentration of  $\text{H}^+$

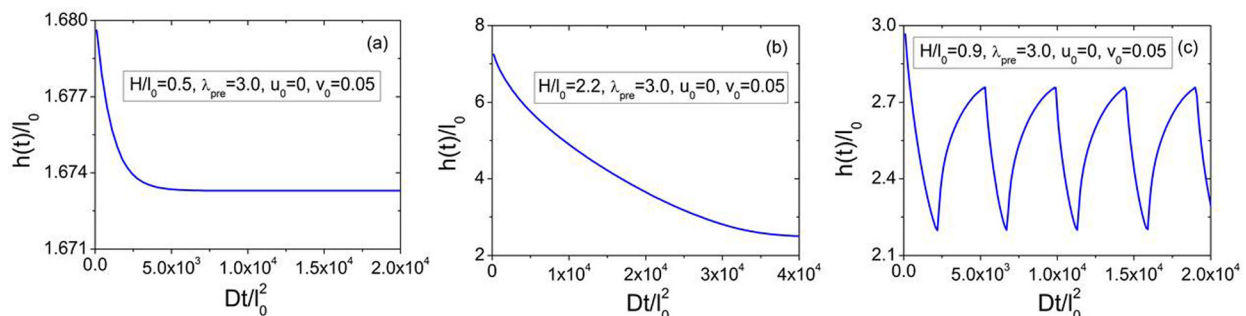


FIG. 2. The evolution of the thickness of the gel layer with different thicknesses in its reference state,  $H$ : (a)  $H/l_0 = 0.5$ , (b)  $H/l_0 = 2.2$ , and (c)  $H/l_0 = 0.9$ . The lateral prestretch is  $\lambda_{pre} = 3.0$ , the initial concentrations of reactants are  $u_0 = 0$  and  $v_0 = 0.05$ , and the corresponding initial vertical stretch in equilibrium is  $\lambda_0 = 3.36$ .

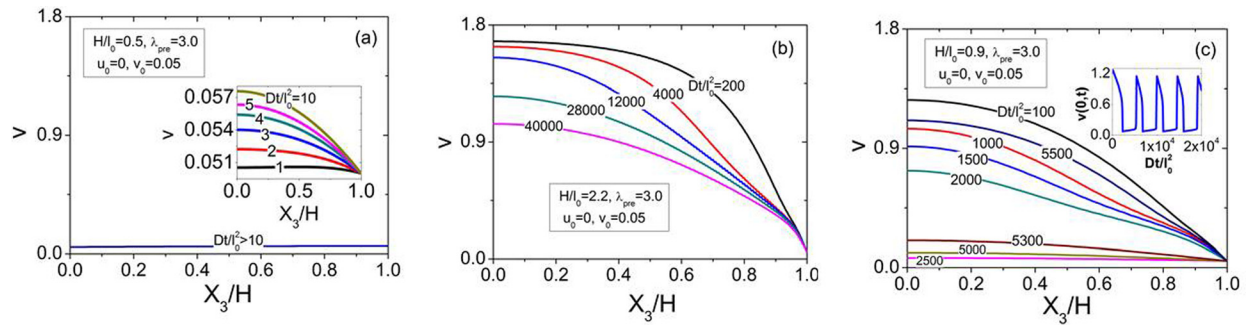


FIG. 3. The evolution of the concentration of  $H^+$  in the gel layer with different thicknesses in its reference state,  $H$ : (a)  $H/l_0 = 0.5$ , (b)  $H/l_0 = 2.2$ , and (c)  $H/l_0 = 0.9$ . Inset in (c) shows the concentration of  $H^+$ , at the bottom of the gel layer, oscillating with time. The lateral prestretches in the gel layer and the initial concentrations of reactants in the gel are the same as those in Figure 2.

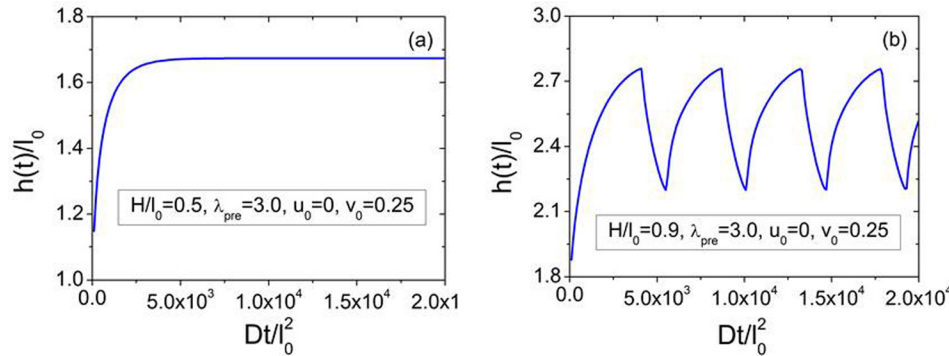


FIG. 4. Influence of the initial concentrations of reactants on the swelling-shrinking behaviors of the gel layer with two different thicknesses: (a)  $H/l_0 = 0.5$  and (b)  $H/l_0 = 0.9$ . We set the initial reactant concentrations in the gel  $u_0 = 0$  and  $v_0 = 0.25$ , which is different from the initial reactant concentrations in the gel in Figure 2.

decreases due to diffusion. After a short period, the gel layer reaches steady state with the same thickness as Figure 2(a). Similarly, in Figure 4(b), we set the gel thickness to be:  $H/l_0 = 0.9$ . Except the early stage of swelling, the thickness of the gel layer in Figure 4(b) oscillates in the same way as shown in Figure 2(c). These two calculations indicate that the initial concentrations of reactants only affect the early stage of swelling-shrinking behaviors of the gel layers but not their long-term behaviors.

In Figure 5, we plot the thickness of the gel changing with time for different lateral prestretches. In Figures 5(a) and 5(b), the thicknesses of two prestretched gel layers in initial state,  $h_0$ , before contacting with the solution are the same, while the prestretches in the gel layers are different. When the prestretch is small,  $\lambda_{pre} = 1.5$ , the gel layer shrinks monotonically with time and, finally, reach steady state (Fig. 5(a)). When the prestretch is large,  $\lambda_{pre} = 3.0$ , the gel layer shrinks first then oscillates and can never reach steady state

(Fig. 5(b)). The time for chemical reactions is independent of the prestretch of the gel, while the time for the diffusion of solvent can quantitatively depend on the deformation of the gel as illustrated in our previous work.<sup>34</sup> Thus, the effect of prestretch on the dynamics of the gel layer can also be understood by considering the effect of prestretch on the time for the diffusion of solvent in the gel layer.

In swelling-shrinking process, the gel layer exerts swelling force on its constrained substrate. The swelling force is often used to trigger deformation of the substrate such as a stiff and nonswellable beam.<sup>39</sup> In these applications, the magnitude of the swelling force is critical. Since the thickness of the gel can change periodically with time in certain conditions (Fig. 2(c)), we expect the magnitude of the swelling force can also oscillate in the same conditions. In Figure 6(a), we plot the lateral stress distribution in the gel layer at different times. The gel layer has the same thickness, lateral prestretches, and initial concentrations of reactants as the

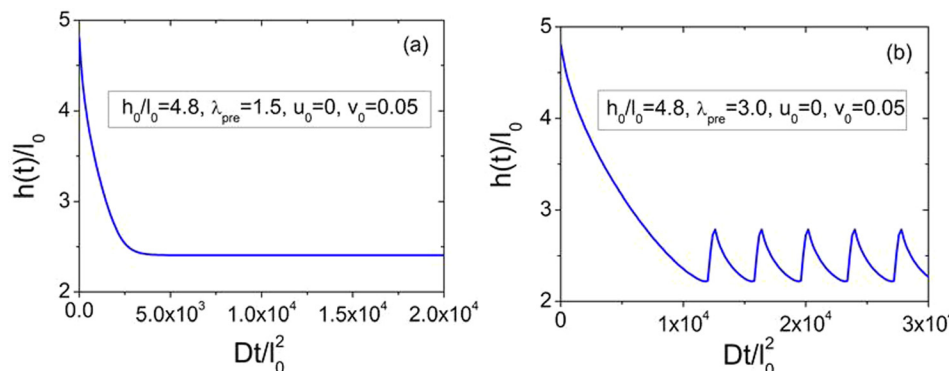


FIG. 5. Influence of the lateral prestretch  $\lambda_{pre}$  on swelling-shrinking dynamics of the gel layer: (a)  $\lambda_{pre} = 1.5$  and (b)  $\lambda_{pre} = 3.0$ . In (a) and (b), the initial thicknesses of two gel layers are the same:  $h_0/l_0 = 4.8$ . The initial reactant concentrations in the gel are  $u_0 = 0$  and  $v_0 = 0.05$ .

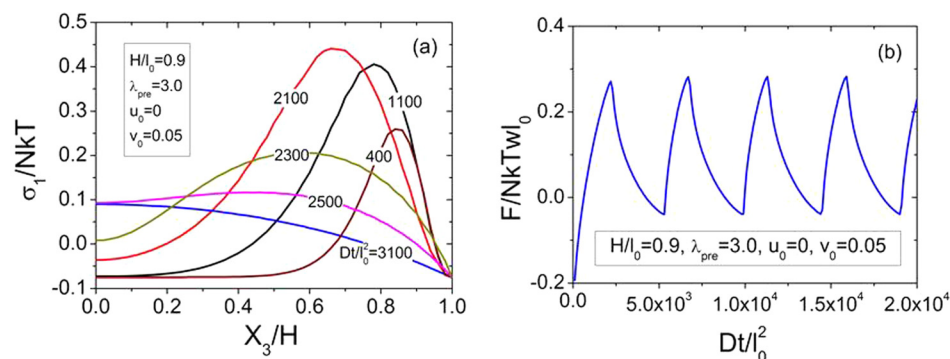


FIG. 6. (a) Distribution of lateral stress  $\sigma_1$  in the gel layer for several times in the oscillation process. (b) The evolution of swelling force  $F$  that the gel layer exerts on the substrate in the oscillation process.

one shown in Figure 2(c). The swelling force  $F$  can be calculated by integrating the lateral stress

$$F(t) = w \int_0^H \sigma_1(X_3, t) \lambda_3(X_3, t) dX_3, \quad (15)$$

where  $w$  is the width of the substrate. As shown in Figure 6(b), the swelling force also oscillates with the same period of the oscillation of the thickness of the gel layer in Figure 2(c).

#### IV. CONCLUSIONS

In conclusion, we investigate the coupling between large deformation and reaction-diffusion of reactants in a constrained gel layer, which is submerged in a continuous stirred tank reactor and an autocatalytic reaction proceeds in it. We illustrate that the dynamic behaviors of the gel layer are determined by its thickness, lateral prestretches, and initial concentrations of reactants. Our calculations show that: in certain conditions, the gel layer in a CSTR can swell or shrink at the beginning and, finally, reach steady state with constant thickness; by changing the initial thickness or the prestretches of the gel layer, the thickness and the swelling force that the gel layer exerts on the constraint may oscillate and the gel never reaches steady state. We have also shown that the oscillating behavior in the gel is the consequence of the coupling between large deformation and reaction-diffusion process of reactants in the gel, which is intrinsically different from BZ self-oscillating gels. The study may find potential applications in designing chemo-mechanical transducers.

#### ACKNOWLEDGMENTS

Kai Li acknowledges the support from Anhui Provincial Natural Science Foundation (Grant No. 1408085QA18). Shengqiang Cai acknowledges the startup funds from the Jacobs School of Engineering at UCSD and Fudan University Key Laboratory Senior Visiting Scholarship.

- <sup>1</sup>Y. Hirokawa and T. Tanaka, *J. Chem. Phys.* **81**, 6379–6380 (1984).
- <sup>2</sup>L. B. Peppas and N. A. Peppas, *Chem. Eng. Sci.* **46**, 715–722 (1991).
- <sup>3</sup>T. Tanaka, I. Nishio, S. T. Sun, and S. U. Nishio, *Science* **218**, 467–469 (1982).

- <sup>4</sup>N. A. Peppas, P. Bures, W. Leobandund, and H. Ichikawa, *Eur. J. Pharm. Biopharm.* **50**, 27–46 (2000).
- <sup>5</sup>D. J. Beebe, J. S. Moore, J. M. Bauer, Q. Yu, R. H. Liu, C. Devadoss, and B. H. Jo, *Nature* **404**, 588–590 (2000).
- <sup>6</sup>R. Langer, *Nature* **392**, 5–10 (1998), available at <http://www.nature.com/nature/supplements/collections/therapeutic/horizons/index.html>.
- <sup>7</sup>R. Shankar, T. K. Ghosh, and R. J. Spontak, *Soft Matter* **3**, 1116–1129 (2007).
- <sup>8</sup>J. A. Pojman and Q. Tran-Cong-Miyata, *Nonlinear Dynamics with Polymers: Fundamentals, Methods, and Applications* (Wiley, 2011).
- <sup>9</sup>R. Yoshida, T. Takahashi, T. Yamaguchi, and H. Ichijo, *J. Am. Chem. Soc.* **118**, 5134–5135 (1996).
- <sup>10</sup>R. Yoshida, M. Tanaka, S. Onodera, T. Yamaguchi, and E. Kokufuta, *J. Phys. Chem. A* **104**, 7549–7555 (2000).
- <sup>11</sup>R. Yoshida, E. Kokufuta, and T. Yamaguchi, *Chaos* **9**, 260–266 (1999).
- <sup>12</sup>K. Miyakawa, F. Sakamoto, R. Yoshida, E. Kokufuta, and T. Yamaguchi, *Phys. Rev. E* **62**, 793–798 (2000).
- <sup>13</sup>R. Yoshida, *Biophysics* **8**, 163–172 (2012).
- <sup>14</sup>S. Maeda, Y. Hara, T. Sakai, R. Yoshida, and S. Hashimoto, *Adv. Mater.* **19**, 3480–3484 (2007).
- <sup>15</sup>A. S. Hoffman, *Adv. Drug Delivery Rev.* **54**, 3–12 (2002).
- <sup>16</sup>V. V. Yashin and A. C. Balazs, *Macromolecules* **39**, 2024–2026 (2006).
- <sup>17</sup>V. V. Yashin and A. C. Balazs, *Science* **314**, 798–801 (2006).
- <sup>18</sup>V. V. Yashin and A. C. Balazs, *J. Chem. Phys.* **126**, 124707 (2007).
- <sup>19</sup>X. Zou and R. A. Siegel, *J. Chem. Phys.* **110**, 2267–2279 (1999).
- <sup>20</sup>G. P. Misra and R. A. Siegel, *J. Controlled Release* **81**, 1–6 (2002).
- <sup>21</sup>A. P. Dhanarajan, G. P. Misra, and R. A. Siegel, *J. Phys. Chem. A* **106**, 8835–8838 (2002).
- <sup>22</sup>V. Labrot, P. De Kepper, J. Boissonade, I. Szalai, and F. Gauffre, *J. Phys. Chem. B* **109**, 21476–21480 (2005).
- <sup>23</sup>T. G. Szántó and G. Rábai, *J. Phys. Chem. A* **109**, 5398–5402 (2005).
- <sup>24</sup>J. Boissonade and P. De Kepper, *Phys. Chem. Chem. Phys.* **13**, 4132–4137 (2011).
- <sup>25</sup>J. Horváth, I. Szalai, and P. De Kepper, *Science* **324**, 772–775 (2009).
- <sup>26</sup>J. Horváth, I. Szalai, J. Boissonade, and P. De Kepper, *Soft Matter* **7**, 8462–8472 (2011).
- <sup>27</sup>M. Fuentes, M. N. Kuperman, J. Boissonade, E. Dulos, F. Gauffre, and P. De Kepper, *Phys. Rev. E* **66**, 056205 (2002).
- <sup>28</sup>J. Boissonade, *Phys. Rev. Lett.* **90**, 188302 (2003).
- <sup>29</sup>J. Boissonade, *Eur. Phys. J. E* **28**, 337–346 (2009).
- <sup>30</sup>K. W. Oh and C. H. Ahn, *J. Micromech. Microeng.* **16**, R13 (2006).
- <sup>31</sup>M. A. Biot, *J. Appl. Phys.* **12**, 155–164 (1941).
- <sup>32</sup>A. C. Shawn and A. Lallit, *J. Mech. Phys. Solids* **58**, 1879–1906 (2010).
- <sup>33</sup>P. J. Flory and J. Rehner, *J. Chem. Phys.* **11**, 521–526 (1943).
- <sup>34</sup>S. Cai, Y. Lou, P. Ganguly, A. Robisson, and Z. Suo, *J. Appl. Phys.* **107**, 103535 (2010).
- <sup>35</sup>R. Marcombe, S. Cai, W. Hong, X. Zhao, Y. Lapusta, and Z. Suo, *Soft Matter* **6**, 784–793 (2010).
- <sup>36</sup>T. Tanaka, D. Fillmore, S. T. Sun, I. Nishio, G. Swislow, and A. Shah, *Phys. Rev. Lett.* **45**, 1636–1639 (1980).
- <sup>37</sup>S. Cai and Z. Suo, *J. Mech. Phys. Solids* **59**, 2259–2278 (2011).
- <sup>38</sup>A. C. Shawn and A. Lallit, *J. Mech. Phys. Solids* **59**, 1978–2006 (2011).
- <sup>39</sup>J. Yoon, S. Cai, Z. Suo, and R. C. Hayward, *Soft Matter* **6**, 6004–6012 (2010).